

ELECTRIC CONDUCTIVITY OF NITROGEN-DOPED DIAMOND-LIKE CARBON FILMS: II. SPACE-CHARGE-LIMITED CURRENTS

A.A. EVTUKH

UDC 539.216,537.222,621.382
© 2009V. Lashkaryov Institute of Semiconductor Physics, Nat. Acad. of Sci. of Ukraine
(41, Nauky Prosp., Kyiv 03028, Ukraine)

The results of experimental investigations of the electric conductivity of nitrogen-doped diamond-like carbon (DLC) films after the thermal annealing are presented. The currents of monopolar injection limited by a volume charge in DLC films annealed at $T = 450$ °C or highly doped with nitrogen are revealed. They are caused by the appearance of deep energy levels (electron traps) in the bandgap of a film at the effusion of hydrogen and at high levels of doping with nitrogen. The concentration of energy traps and their energy position in the bandgap of DLC (a-C:H) films after the thermal annealing or the high-dose doping with nitrogen are determined. The deep energy trap concentration is in the range $(3 \times 10^{17} - 5 \times 10^{18}) \text{ cm}^{-3}$ and has a nonmonotonous dependence on the doping level with nitrogen. Energy levels are lower by (0.11–0.55) eV than the conduction band bottom. Two energy levels positioned at different depths are observed for some films.

and content of films. That is why the investigation of the electrophysical properties of DLC films should tightly correlate with a technology of their preparation and other physical properties. For the wide application of DLC films in devices of both solid state and vacuum micro- and nanoelectronics, it is necessary, first of all, to investigate their electrophysical properties, among which the current transport mechanism being the most important.

In this work, the results of experimental investigations of the electrical conductivity of hydrogen-enriched DLC films (a-C:H) after the thermal annealing are presented. The current transport mechanism will be established, and the energy position of electron traps in the forbidden band and their density will be determined.

1. Introduction

Diamond-like carbon (DLC) films are a metastable form of amorphous carbon that has a significant part of sp^3 bonds and are referred to amorphous semiconductors. Carbon creates a wide variety of crystalline and disordered structures due to its possibility to form three types of hybrid bonds, namely sp^3 , sp^2 , and sp^1 [1,2].

There are many achievements in investigations of the influence of the disordering in amorphous semiconductors on their energy band structure and electron properties [3–5]. Some models of energy dependence of the electron state density assuming both the existence of localized energy states in “tails” of the valence and conduction bands, and the threshold of mobility that separates delocalized and localized states are proposed.

Nevertheless, despite the great number of works devoted to investigations of the electrophysical properties of DLC films, no complete ideas of and knowledge about the current transport mechanisms, charge characteristics, energy barrier heights at interfaces, *etc.* are available. First of all, this is caused by the strong dependence of electrophysical properties on the sp^3/sp^2 atom bond configuration ratio, structure,

2. Experimental

In our experiments, the technology of fabrication of DLC film by the plasma enhanced chemical vapor deposition (PE CVD) method has been optimized, and the influence of technological conditions (the content of a gas mixture, pressure in a reaction chamber, *etc.*) on properties, first of all electrophysical ones, of DLC films has been investigated. DLC films were grown on flat silicon wafers by the PE CVD method from the gas mixture $\text{CH}_4:\text{H}_2$; $\text{CH}_4:\text{H}_2:\text{N}_2$. On the deposition of DLC films, the high frequency generator with a power of 2.5 kW and a frequency of 13.56 MHz was used. Among variable parameters were the flow of gases (CH_4 , H_2 , N_2), their content in the mixture, and the total pressure of the mixture.

The films obtained by the PE CVD method from hydrocarbons have a high content of hydrogen. Its concentration depends on deposition process parameters [6]. The hydrogen content can reach 30–40% in “hard” a-C:H films and even up to 40–50% in “soft” a-C:H films [6, 7].

Hydrogen builds in the amorphous carbon matrix on dangling carbon bonds and/or at the creation of the

polymer part of a film [6, 8]. In this relation, hydrogen plays a critical role in the bond configuration of carbon atoms. It promotes the stabilization of the tetrahedral sp^3 configuration and, respectively, plays a significant role in the determination of both the electrical and optical properties of a-C:H films. The part of hydrogen in the a-C:H films can be found in the interstitial non-bonding state [9, 10].

During the PE CVD fabrication of DLC films from the mixture of CH_4 , H_2 , and N_2 , the nitrogen content was changed from 0 to 45%. The gas mixture pressure in a vacuum chamber that had discrete values 0.2, 0.6 and 0.8 Torr was as a parameter. The nitrogen influence analysis was performed in comparison with properties of undoped DLC films deposited with the $\text{CH}_4:\text{H}_2$ mixture. As Auger electron spectroscopy results [11] show, there is a correlation between the nitrogen concentration in the gas mixture and its content in a DLC film. After the deposition and measurements of the characteristics of DLC films, they were annealed at $T = 450^\circ\text{C}$ for 60 min in argon.

To investigate the electric conductivity of DLC films (a-C:H), the metal-insulator-semiconductor structure (MIS) with a DLC film instead of an insulator was formed. DLC films were deposited on a silicon wafer of the n - or p -type with the specific resistivity $\rho_v = 4.5$ Ohm-cm or $\rho_v = 10$ Ohm-cm, respectively. After the deposition of a DLC film, the aluminum electrodes with a thickness of $(0.8\text{--}1.0)$ μm were formed by the resistive deposition through a mask. The area of the separate upper electrode (capacitor) was 8×10^{-3} cm^2 . To realize the reliable contact, the overall aluminum electrode was sputtered on the back side of a silicon wafer.

In such structures, the current-voltage ($I - V$) characteristics were measured with an automatic setup Hewlett-Packard Analyzer 4145A for the investigation of peculiarities of the current transport. To exclude the influence of the substrate on $I - V$ characteristics of DLC films, the voltage with polarity corresponding to the accumulation of majority carriers on the silicon substrate surface was applied. The dark current measurements were performed at room temperature (293 K).

3. Results and Discussion

We measured the $I - V$ characteristics of the monopolar injection that are characteristic of space-charge-limited currents (SCLC) [12] through a-C:H films highly doped with nitrogen ($N_2 = 45\%$) and those annealed at $T = 450^\circ\text{C}$ in Ar (undoped and doped). The important peculiarity of such $I - V$ characteristics is a sharp growth

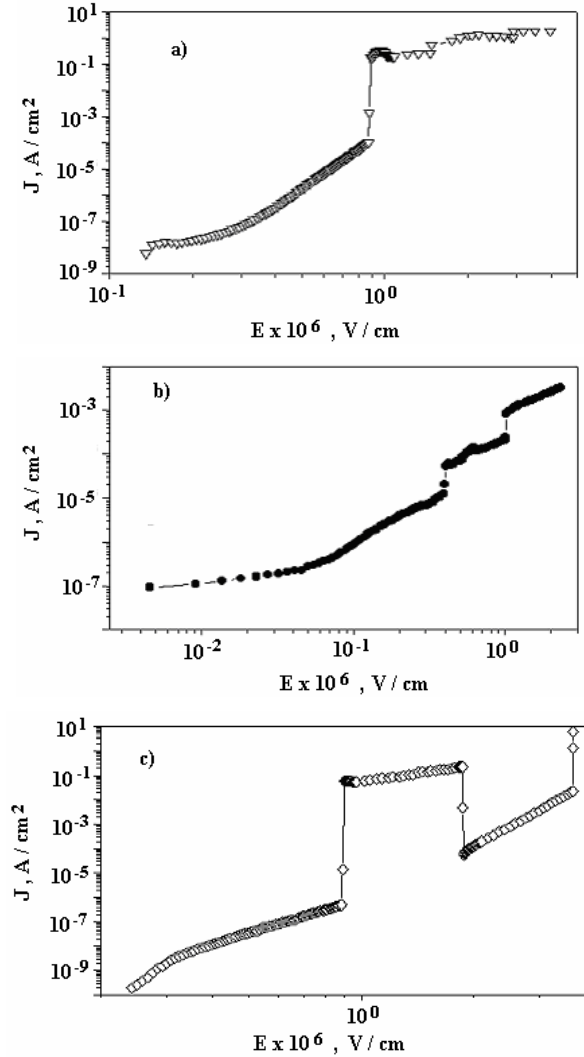


Fig. 1. Space-charge-limited currents in annealed and highly nitrogen-doped DLC films ($P = 0.2$ Torr): a) $I - V$ characteristics of films with one electron trap level ($N_2 = 20\%$); b) $I - V$ characteristics of the films with two electron trap levels ($N_2 = 45\%$); c) $I - V$ characteristics in the case of the combined electron transport mechanism ($N_2 = 10\%$)

of the current (up to 6 orders) at definite values of the electric field. As a rule, there are three distinct regions in $I - V$ characteristics (Fig. 1), namely the regions corresponding to (i) the Ohm law or the square law with traps, (ii) the full filling of traps (sharp vertical growth of current), and (iii) the square law without traps.

The change of the behavior of $I - V$ characteristics of annealed DLC films is caused by the output (effusion) of hydrogen from films at the annealing. It is known that

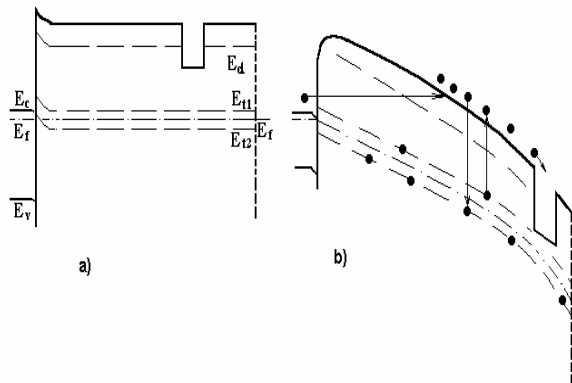


Fig. 2. Energy band diagram fragments of Si-DLC films and the current transport mechanisms in the case of structures with annealed or highly nitrogen-doped DLC films: a) without electric field; b) at an applied electric field

hydrogen significantly influences the electrical properties of semiconductors. It passivates the broken bonds in amorphous silicon [3, 13], grain boundaries in polycrystalline silicon [14], donor and acceptor impurities in single crystal silicon [15], and shallow impurities in GaP [16]. In a number of works [17–19], the significant influence of hydrogen on the electric conductivity of diamond and diamond films was demonstrated.

The electric conductivity of an amorphous semiconductor is determined by the density of states, mobility of carriers, and their distribution over electron states. For example, films of hydrogen-free amorphous silicon have a very high density of states in the forbidden band caused by defects. Therefore, the conductivity is determined by the hopping mechanism in the Fermi level region. In hydrogen-containing films of amorphous silicon a-Si:H, the density of defects is significantly lower, and the conductivity is determined by the electron and hole hopping on the edges of bands, where the density of state and mobility increase with the energy. The method of preparation of amorphous semiconductors determines details of the film structure and their defectiveness and influences significantly the conductivity. By studying the hydrogen evolution at the thermal annealing of hydrogen-containing amorphous semiconductors, it was shown that the output of hydrogen in a-Si:H films begins at the annealing temperature $T = 350$ °C. At $T = 550$ °C, the more than 80% of hydrogen left the films [20]. In the case of a-Si_{1-x}Ge_x:H films, hydrogen leaves the films at >300 °C [21]. The output of hydrogen from a-Si_{1-x}C:H films was observed at $T = 350$ – 400 °C [22]. The output

of hydrogen from amorphous semiconductors causes the creation of broken (dangling) bonds. As a rule, a decrease of the film thickness and an increase of the density are observed at the annealing. This indicates a transformation of the structure and the composition of the films.

DLC films at the thermal annealing show main regularities that are characteristic of other amorphous semiconductors. It was shown in work [23] that the annealing at $T > 300$ °C causes a reconstruction of the DLC film structure: a decrease of both the ratio of sp^3/sp^2 configurations of bonds in the film and the optical bandgap is observed.

DLC (a-C:H) films investigated by us after the deposition were enriched by hydrogen, since the deposition was performed from the mixture of CH₄, H₂, and N₂. The enrichment of amorphous films by hydrogen is characteristic of chemical vapor deposition processes with hydrogen-containing gases. As a result, the defect centers are passivated by hydrogen, i.e. hydrogen cures broken bonds. It leads to a reduction of the number of the electron states in the forbidden band of the material. In addition, hydrogen promotes the creation of the sp^3 configuration of atom bonds [24]. At the annealing, hydrogen leaves the films, and structural defects of a film create the local electron states in the forbidden band. This causes the changing of the electric conductivity mechanisms.

In the case of highly nitrogen-doped films, their I – V characteristics are similar to those of annealed DLC films and corresponds to SCLC. But the nature of the creation of energy states in the forbidden band of a DLC film is quite different. At the introduction of nitrogen, it builds firstly into the film structure in the ionized state, by creating donor centers. But, with increase of the nitrogen concentration, it begins to build in a nonactive state with the creation of deep traps in the middle region of the forbidden band (Fig. 2). The initial growth of the electric conductivity with its following lowering is observed at the increase of the nitrogen concentration in the film. Under a significant increase of the concentration of traps in the forbidden band, the electric conductivity according to the SCLC mechanism is revealed.

The analysis of I – V characteristics corresponding to the SCLC mechanism of conductivity allowed us to determine the concentration and the energy position of traps.

If the current vs. voltage dependence built in double logarithmic coordinates has a sharp vertical region, it is caused by the filling of monoenergetic sticking levels (electron traps). The shape of the I – V characteristic in

Fig. 1, *a* is typical of the monopolar injection of charge carriers. It is possible to write the following expression for the electric field (E_{tfl}) corresponding to the sharp increase of the current in the case of deep traps [12]:

$$E_{tfl} = \frac{e \times p_{t0} \times d}{2\varepsilon_d \varepsilon_0}. \quad (1)$$

Here, e is the electron charge, $\varepsilon_d \varepsilon_0$ is the static dielectric permeability, d is the film thickness, and p_{t0} is the concentration of traps unfilled by electrons on a level E_t .

If several critical fields corresponding of the full filling of related energy levels are observed on $I - V$ characteristics, the electrical conductivity is realized with the participation of several energy levels. The quantity p_{t0} in Eq. (1) can be presented as

$$p_{t0} = N_t - n_{t0} = \frac{N_t}{1 + g \exp\left(\frac{E_{F0} - E_t}{kT}\right)} \approx \frac{N_t}{g} \exp\left(\frac{E_t - E_{F0}}{kT}\right), \quad (2)$$

where N_t is the total concentration of traps, n_{t0} is the concentration of filled traps, and g is the spin degeneration coefficient (statistical weight).

If the almost vertical region on the $I - V$ characteristic is directly preceded by the square-law region, it is possible to conclude that the energy levels (sticking levels) are located significantly higher of the equilibrium Fermi level E_{F0} . That is, the condition $(E_t - E_{F0})/kT \gg 1$ is satisfied, and therefore all levels are empty in the initial state, i.e. $p_{t0} = N_t$.

If the almost vertical region on the $I - V$ characteristic is directly preceded by the linear-law region, it is known only that the sticking levels are located on the E_{F0} level or lower than it, i.e. the condition $(E_{F0} - E_t)/kT \geq 1$ is satisfied. Thus, it is possible to determine only the lower border for N_t , namely $N_t \geq p_{t0}$.

The measurements of SCLC give possibility to obtain not only the concentration of traps but also the information about the depths of energy levels in the forbidden band, E_t .

If the almost vertical region of the $I - V$ characteristic corresponding to the full filling of traps is directly preceded by the square-law region, then the last one has to be defined by the "trap" square law [12]

$$J = 9/8 \times \theta \times \varepsilon_d \varepsilon_0 \times \mu \times \frac{E^2}{d}. \quad (3)$$

It corresponds to the same group of sticking levels N_t . This branch of the curve lgJ versus lgE is positioned lower than the line of the "trapless" square law

$$J = 9/8 \times \varepsilon_d \varepsilon_0 \times \mu \times \frac{E^2}{d} \quad (4)$$

at the distance equal to θ that is determined by the formula

$$\theta = \frac{n}{n_t} = \frac{n_0 + n_i}{n_t} = \frac{p}{p_t} = \frac{N}{gN_t} = \frac{N_c}{gN_t} \exp\left(\frac{E_t - E_c}{kT}\right). \quad (5)$$

After the determination of the concentration N_t with the use of ratio (1), the quantity E_t is calculated by the relation

$$E_c - E_t = kT \ln \frac{N_c}{\theta g N_t}. \quad (6)$$

To calculate theoretically θ , it is necessary to know ε_d and μ . Whereas, for the determination of E_t , the values of N_c and g have to be known, though large deviations from $g = 2$ are improbable.

It is possible to determine E_t experimentally from the shift θ of one square-law region of the $I - V$ characteristic relative to another one. From relations (3) and (4), we obtain

$$\theta = J_1/J_0, \quad (7)$$

where J_1 and J_0 are the currents corresponding to the "trap" and "trapless" square laws, respectively, at the point of the critical electric field (the full filling of traps).

The other important case is when the ohmic region directly precedes the branch of the $I - V$ characteristic corresponding to the "trap" square law. Then θ is determined from the point E_x of the intersection of two mentioned regions presented on the double logarithmic scale at their extrapolation. The expression for θ has the form

$$\theta = \frac{e \times n_0 \times d}{\varepsilon_d \varepsilon_0 \times E_x}. \quad (8)$$

According to the above-presented analysis, we determined N_t and E_t for DLC films annealed in Ar at $T = 450$ °C and for films highly doped with nitrogen.

The obtained experimental values of N_t and E_t are presented in Table 1 and in Fig. 3. As seen, the electron trap concentration is in the range $3 \times 10^{17} \text{ cm}^{-3} - 5 \times 10^{18} \text{ cm}^{-3}$ and has a nonmonotonous dependence on the nitrogen doping level with the maximum value

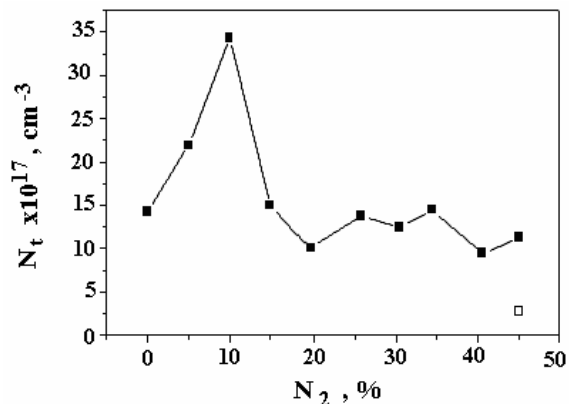


Fig. 3. Deep electron trap concentration in the forbidden band of DLC films after the annealing ($T = 450$ °C, $t = 60$ min in Ar) versus the nitrogen content at the deposition (\square – without annealing)

at $N_2=10\%$. The existence of two local energy levels was revealed in some films ($N_2 = 10\%$, 25% , 35% , 40% , 45%). The energy levels are placed by 0.11 to 0.39 eV lower than the conduction band bottom. The E_t vs. N_2 dependence is nonmonotonous with the minimal value $E_t = 0.11$ eV at $N_2 = 30\%$. In the case of a DLC film highly doped with nitrogen ($N_2 = 45\%$) without annealing, $E_t = 0.55$ eV.

The comparative analysis of the currents through DLC films before (J_0) and after (J_a) the annealing on the initial part of the $I - V$ characteristic shows their ambiguous relationship, namely $N_2=0\%$, 15% , 20% , $J_0 \approx J_a$; $N_2 = 5\%$, 10% - $J_0 > J_a$; $N_2 \geq 25\%$ $J_0 < J_a$. Such ambiguous relationships of J_0 and J_a are caused not only by the electron trap creation during the annealing, but also by the structural reconstruction of the films.

The growth of the refractive index also indicates the structural reconstruction. The ratio of the refractive index of annealed DLC films n_a to that of nonannealed ones n_o is shown in Fig. 4,a. The ratio n_a/n_o increases with the nitrogen concentration. The data obtained by us are in good agreement with the data of other authors for amorphous semiconductors. The increase of the refractive index after the thermal annealing of a-Si:H and a-Si_{1-x}C_x:H films was observed in work [22]. The data of work [23] also point out to the structural reconstruction in a-C:H films during the thermal annealing. A decrease of both the sp^3/sp^2 ratio and the optical bandgap was observed with increase of the annealing temperature [23]. A decrease of the optical bandgap with increase of the annealing temperature was also observed for a-Si:H and a-Si_{1-x}C_x:H films [22].

The dependences the electric conductivity of DLC films on the nitrogen content in a gas mixture at their PE CVD deposition before and after the thermal annealing are presented in Fig. 4,b. The electric conductivity was determined at the electric field strength $E = 1 \times 10^6$ V/cm in films at room temperature. No monotonous dependence of the electric conductivity σ on the nitrogen content is observed. The electric conductivity increases sharply at low N_2 concentrations (5% , 10%). But the subsequent growth of the N_2 concentration leads to its gradual decrease to values close to one for DLC films undoped with nitrogen. The electric conductivity of the DLC films under study was in the range of $(10^{-15}-10^{-9})$ $\text{Ohm}^{-1}\cdot\text{cm}^{-1}$. It is in good agreement with values of σ for a-C:H from the literature [25]. The low electric conductivity of a-C:H films is caused by the high content of hydrogen that blocks broken bonds and decreases, in such a manner, the concentration of traps, which take part in the current transport, in the forbidden band. At the same time, it is known that the electric conductivity of a-C films (without hydrogen) is higher significantly $\sigma = 1 \times 10^{-4}$ $\text{Ohm}^{-1}\text{cm}^{-1}$ [26]. As seen from Fig. 4,b, the thermal annealing in the case of higher nitrogen doping levels causes a significant growth of the electric conductivity (up to 3 orders).

The experimental results give evidence of the structural reconstruction of films that causes the changing of the energy bandgap along with the creation of energy levels in the bandgap due to the effusion of hydrogen. The appearance of additional energy levels and a change of E_g cause the complicated character of changes in the current transport through DLC films.

The $I - V$ characteristics corresponding to SCLC with the presence of vertical sections with the sharp growth of the current, which are typical of the case of the full filling of traps on the E_t level, were observed for

Table 1. Concentration and the energy position of electron traps in nitrogen-doped DLC films after the thermal annealing ($T = 450$ °C, $t = 60$ min Ar)

N_2 , %	$N_{t1} \times 10^{17}$, cm^{-3}	$N_{t2} \times 10^{17}$, cm^{-3}	E_{t1} , eV	E_{t2} , eV
0	≥ 14.3	–	–	–
5	21.9	–	–	–
10	6.7	27.6	0.39	–
15	≥ 15	–	–	–
20	6.6	–	0.30	–
25	3.6	13.2	0.23	–
30	12.5	–	0.11	–
35	4.2	14.1	0.33	–
40	3.5	4.5	0.38	0.29
45	3.3	8.0	0.19	0.17
45*	2.8	–	0.55	–

* – without annealing

all annealed DLC films. In the case of DLC films deposited at a high nitrogen concentration and annealed in argon, two regions corresponding to the full filling of traps were observed on the $I - V$ characteristics (Fig. 1, *b*). This points out to the existence of two types of monoenergetic levels with different energies in a film after the annealing. Two types of levels correspond to different structure defects. One energy level is caused by nitrogen built in the inactive (nonionized) state, and another one is related to the creation of defects (broken bonds) at the hydrogen effusion from a film. In the case of annealed films with a lower value of the nitrogen concentration ($N_2=5-30\%$), the $I - V$ characteristics indicating the existence of a single clearly pronounced monoenergetic level in the bandgap of a DLC film are observed. Along with the sharp growth of the current corresponding to the full filling of traps at SCLC, the regions with a sharp decrease of the current were revealed in the $I - V$ characteristics of the films highly doped with nitrogen ($N_2=45\%$) and the annealed films previously doped with nitrogen at $N_2=0\%$, 10% and 35% (Fig. 1, *c*). To explain these dependences, it is necessary to take two mechanisms of current transport through DLC films into account, namely SCLC and the current transport by the hopping transport mechanism or by the Poole-Frenkel mechanism in the case of a narrower bandgap and shallower traps.

So, the space-charge-limited currents were observed for DLC films after the low-temperature annealing and in the case of high nitrogen doping levels. In such DLC films, the important role is played by deep energy levels in the bandgap.

4. Conclusion

The currents of the monopolar injection limited by the volume charge in DLC films annealed at $T=450^\circ\text{C}$ or films highly doped with nitrogen are revealed. They are caused by the appearance of deep energy levels (electron traps) in the bandgap of a film at the effusion of hydrogen and at high levels of doping with nitrogen.

The concentration of energy traps and their energy position in the bandgap of DLC (a-C:H) films after the thermal annealing or the high-level doping with nitrogen are determined. The deep energy trap concentration is in the range $(3 \times 10^{17} - 5 \times 10^{18}) \text{ cm}^{-3}$ and has a nonmonotonous dependence on the nitrogen doping level. Energy levels are placed lower by $(0.11 - 0.55) \text{ eV}$ than the conduction band bottom. Two energy levels positioned at different depths were observed for some films.

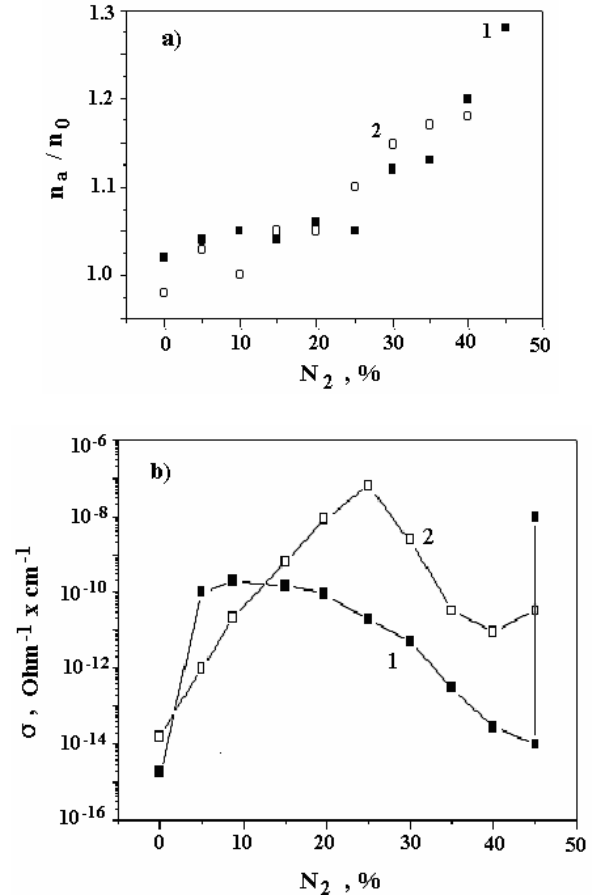


Fig. 4. Ratio of the refraction indices (*a*) and the dark electric conductivities (*b*) of DLC films after and before the thermal annealing versus the nitrogen content: (*a*) 1 – $P = 0.2$ Torr, 2 – $P = 0.6$ Torr; (*b*) before (1) and after (2) thermal annealing ($P = 0.2$ Torr)

This work was supported by the Projects of the STCU No. 3819, the Ministry of Education and Science of Ukraine No. M/175-2007, and the NASU No. 44/E5.4.

1. J. Robertson, *Mater. Sci. and Engin.* **R37**, 129 (2002).
2. N.N. Pavlov, *Theoretical Foundations of General Chemistry* (Vyssh. Shkola, Moscow, 1978) (in Russian).
3. N.F. Mott and E.A. Davis, *Electron Processes in Non-Crystalline Materials* (Clarendon Press, Oxford, 1979).
4. A.K. Jonscher and R.M. Hill, in *Physics of Thin Films*, edited by G. Hass, M.H. Francombe, and R.W. Hoffman (Acad. Press, New York, 1975), Vol. 8, p. 155.
5. *Amorphous Semiconductors*, edited by M.H. Brodsky (Springer, Berlin, 1979).
6. B. Dischler, A. Bubenzer, and P. Koidl, *Appl. Phys. Lett.* **42**, 636 (1983).

7. M. Weiler, S. Sattel, K. Jung, and H. Ehrhardt, *Appl. Phys. Lett.* **64**, 2797 (1994).
8. N. Savvides, *J. Appl. Phys.* **55**, 4232 (1984).
9. C. Donnet, J. Fontaine, F. Lefebvre, A. Grill, V. Patel, and C. Jahnes, *J. Appl. Phys.* **85**, 3264 (1998).
10. A. Grill and V. Patel, *Appl. Phys. Lett.* **60**, 2089 (1992).
11. A.A. Evtukh, V.G. Litovchenko, N.I. Klyui, R.I. Marchenko, and S.Yu. Kudzinovski, *J. Vac. Sci. Technol.* **B17**, 679 (1999).
12. M.A. Lampert and P. Mark, *Current Injection in Solids* (Acad. Press, New York, 1970).
13. J.I. Hanoka, C.H. Seager, D.J. Sharp, and J.K.G. Panitz, *Appl. Phys. Lett.* **42**, 618 (1983).
14. R.C. Eden, *Rev. Sci. Instrum.* **41**, 252 (1970).
15. S.J. Pearton and A.J. Tavendale, *J. Appl. Phys.* **54**, 1375 (1983).
16. M. Singh and J. Weber, *Appl. Phys. Lett.* **54**, 424 (1989).
17. M.I. Landstrass and K.V. Ravi, *Appl. Phys. Lett.* **55**, 975 (1989).
18. M.I. Landstrass and K.V. Ravi, *Appl. Phys. Lett.* **55**, 1391 (1989).
19. S. Albin and L. Watkins, *Appl. Phys. Lett.* **56**, 1454 (1990).
20. M. Hirose, in *Amorphous Semiconductor Technologies and Devices* (OHMSHA, Tokyo; North-Holland, Amsterdam, 1983), Vol. 6, P.173.
21. L. Battezzati, F. Demichelis, C.F. Pirri, and E. Tresso, *J. Appl. Phys.* **69**, 2029 (1991).
22. T. Stapinski, *Amorphous and Microcrystalline Silicon-Based Alloys for Device Applications* (Wydawn. Naukowo-Dydaktyczne, Krakow, 1999).
23. B. Dischler, A. Bubenzer, and P. Koidl, *Solid State Commun.* **48**, 105 (1983).
24. J.C. Angus, *Thin Solid Films* **216**, 126 (1992).
25. T. Mori and Y. Namba, *J. Vac. Sci. Technol.* **A1**, 23 (1983).
26. H. Tsai and D.B. Bogy, *J. Vac. Sci. Technol.* **A5**, 3287 (1987).

Received 15.04.08

ЕЛЕКТРОННА ПРОВІДНІСТЬ ЛЕГОВАНИХ АЗОТОМ
АЛМАЗОПОДІБНИХ ВУГЛЕЦЕВИХ ПЛІВОК:
II. СТРУМИ, ОБМЕЖЕНІ ОБ'ЄМНИМ ЗАРЯДОМ

A.A. Євтух

Резюме

В даній роботі наведено результати експериментальних досліджень електропровідності алмазоподібних вуглецевих (АПВ) плівок, легованих азотом після термічного відпалу. Виявлено струми монополярної інжекції, обмежені об'ємним зарядом в АПВ-плівках, відпалених при $T = 450$ °C та сильнолегованих азотом. Вони зумовлені появою глибоких енергетичних рівнів (електронних пасток) в забороненій зоні плівки під час ефузії з неї водню і при високих рівнях легування азотом. Визначено концентрацію електронних пасток та їх енергетичне положення в забороненій зоні АПВ-плівок, збагачених воднем (а-С:Н) після їх термічного відпалу і високодозового легування азотом. Концентрація глибоких електронних пасток знаходиться в діапазоні $(3 \cdot 10^{17} - 5 \cdot 10^{18})$ см⁻³ і має немонотонну залежність від рівня легування плівок азотом. Енергетичні рівні розміщені в діапазоні (0,11–0,55) еВ нижче дна зони провідності. Для деяких плівок спостерігали два енергетичні рівні, розміщені на різній глибині.